Editors' Suggestion

Improved Phase Locking of Laser Arrays with Nonlinear Coupling

Simon Mahler,[1,*] Matthew L. Goh,[1,2] Chene Tradonsky,[1] Asher A. Friesem,[1] and Nir Davidson[1]
[1]Department of Physics of Complex Systems, Weizmann Institute of Science, Rehovot 761001, Israel
[2]Department of Quantum Science, RSPhys, The Australian National University, Canberra ACT 0200, Australia

(Received 11 October 2019; accepted 24 February 2020; published 1 April 2020)

An arrangement based on a degenerate cavity laser for forming an array of nonlinearly coupled lasers with an intracavity saturable absorber is presented. More than 30 lasers were spatially phase locked and temporally Q switched. The arrangement with nonlinear coupling was found to be 25 times more sensitive to loss differences and converged five times faster to the lowest loss phase locked state than with linear coupling, thus providing a unique solution to problems that have several near-degenerate solutions.

DOI: 10.1103/PhysRevLett.124.133901

Phase locking of lasers corresponds to a state where all the lasers have the same frequency and the same constant relative phase, leading to a coherent superposition of their fields [1,2]. Accordingly, the total brightness of the lasers is high and allows focusing of all the lasers to a sharp spot [3–5]. Phase locking of lasers has been incorporated in many investigations, including simulating spin systems [6–9], finding the ground-state solution of complex landscapes [6,9,10], observing dissipative topological defects [11,12], and solving the phase retrieval problem [13].

Phase locking of laser arrays can be achieved with dissipative coupling that leads to a stable state of minimal loss, which is the phase locked state [6,11,12]. Dissipative coupling involves mode competition whereby modes of different losses compete for the same gain [2,6,9,14]. Only modes with the lowest loss survive and are amplified by the gain medium. Accordingly, by inserting amplitude and phase linear optical elements into a laser cavity that minimize the loss of the phase locked states, it is possible to achieve phase locking with mode competition [2–4,15].

While phase locking with such linear optical elements has yielded many exciting results [4–6,9,11,13–18], it suffers from inherent limitations. It is very sensitive to imperfections, such as positioning errors, mechanical vibrations, thermal effects and other types of aberrations associated with these intracavity elements. Moreover, in many cases, especially for spin simulations and computational problem solving [6,10,13,19], there are two or more states with nearly degenerate minimal loss that cannot be distinguished from each other.

In this Letter, we resort to nonlinear coupling between lasers by means of a saturable absorber (SA). A SA is a nonlinear optical element that block light until it saturates, where its optical loss decreases sharply [20]. It can thus affect the temporal modes within the laser so as to obtain passive Q switching and (longitudinal) mode locking, for generating short pulses and high output peak powers [1] and studying nonlinear laser dynamics [1,3,21–23]. Nonlinear coupling with SA in the spatial domain was used to phase lock two lasers [3] and for selecting spatial modes [24,25]. Here we analyze and demonstrate that a SA can robustly and efficiently phase lock many lasers. Specifically, inserting a SA at the far-field plane of a laser array ensures that the phase locked state (that has sharp and strong intensity peaks there [3–6,19]) corresponds to the minimal loss state, to be selected by optical feedback (mode competition) [18].

We show experimentally and numerically that nonlinear coupling provides stable phase locking and is inherently more robust to alignment errors, aberrations and noise than linear coupling. Moreover, nonlinear mode coupling provided by the SA both in the spatial and temporal domains can yield multiple coupled copies of the laser array (corresponding to different longitudinal modes) that all converge to the same minimal loss state. Hence, significantly improving the ability of the coupled lasers to distinguish between near-degenerate states.

Our experimental arrangement with nonlinear coupling of laser arrays is based on a degenerate cavity laser (DCL) [4,5,26], schematically presented in Fig. 1(a). It was comprised of two flat mirrors where one served as a back mirror with high 99.5% reflectivity and the other as an output coupler with 80% reflectivity. A mask of holes for forming the array of lasers was placed at the near-field plane, adjacent to the output coupler. In our investigations, the mask was a square array of holes of diameter 200 μm and period $a = 300$ μm. The gain medium was Nd:YAG crystal rod of 0.95 cm diameter and 10.9 cm length placed adjacent to the back mirror and optically pumped by quasi-CW 100 μs pulsed flash lamps operating at 1 Hz flashing pulse rate, so operating wavelength is $\lambda = 1064$ nm. Between the mirrors, two spherical (Fourier) lenses of focal lengths $f = 20$ cm and diameters 5.08 cm formed a $4f$ telescope configuration. Due to the $4f$ telescope, each hole in the mask was precisely imaged onto itself after a cavity round-trip, to obtain an independent laser.

The nonlinear coupling between the lasers was achieved with a Cr:YAG saturable absorber, having initial transmission of 45%, which was inserted in the far-field (Fourier) plane midway between the two lenses of the $4f$ telescope [4,5]. For comparison, we also performed experiments with linear coupling by removing the SA and displacing the output coupler by half of the Talbot length from the mask, such that the round-trip distance between them (Talbot distance) is equal to the Talbot length $Z_T = (2a^2/\lambda)$ and the cavity length becomes $4f + Z_T/2$ [5] [27].

First, we detected the time evolution of the laser array output power without and with the SA. Figure 1(b) shows the results without the SA where the lasing pulse duration was 200 μs with complicated strong oscillations. Figure 1(c) shows the results with the SA where the lasing pulse duration was reduced to 100 ns indicating temporal Q switching [1]. The total energy in both cases was similar.

Next, we characterized the spatial coherence between the lasers by measuring the near-field and far-field intensity distributions without and with the SA. The lasers were operated close to their lasing threshold. As evident in Fig. 2, the near-field intensity distributions of the square array of lasers are essentially the same, while the far-field intensity distributions differ dramatically, indicating different spatial coherences. Specifically, the broad Gaussian in the far-field intensity distribution without the SA in Fig. 2(a) indicates no phase relation between the different lasers in the array [3–5].

On the other hand, the sharp peaks in the far-field intensity distribution with the SA in Fig. 2(b) indicate in phase locking of most, if not all, of the 30 lasers in the array [3–5]. These high intensity peaks increase the saturation of the SA and minimize loss. This minimal nonlinear loss combined with mode competition explain the phase locking mechanism of the lasers by the SA. Even more lasers can be phase locked with the SA, but with a somewhat lower quality [27]. We also performed numerical simulations to support our experimental results. The simulations were performed by combining the Fox-Li algorithm [30] and the Gerchberg-Saxton algorithm [31] to obtain a combined algorithm [5]. As evident in Fig. 2, the simulated far-field intensity distributions are in good agreement with the experimental ones, indicating that the SA phase locked the lasers in the in phase state.

For some pump pulse realizations, other phase locked states such as the out of phase state [3–5] can occur. The other phase locked states also have sharp peaks in their far-field intensity distribution and similarly minimize loss. Some typical results are presented in Fig. 3, showing experimental far-field intensity distributions with a SA for different pump pulse realizations. Figures 3(a) and 3(b) show the in phase and out of phase states, and Fig. 3(c) shows a coexistence state of the in phase and out of phase states. To explain such a coexistence state, we note that each laser in the array contains several hundreds of temporal (longitudinal) modes [5,6]. Each of these longitudinal modes corresponds to a different realization of the spatially coupled lasers so phase locking could be either in the in phase state or in the out of phase state. In the coexistence state, part of the longitudinal modes phase locked in phase and part out of phase [5,6].

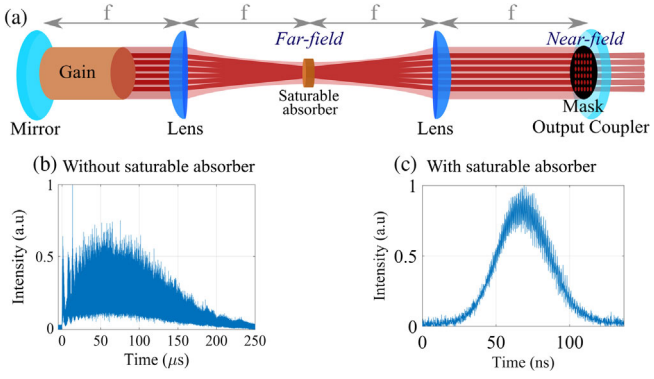

FIG. 1. Degenerate cavity laser (DCL) arrangement and experimental temporal evolution of the laser array intensity. (a) DCL arrangement with a mask of holes in the near-field plane so as to form an array of lasers and a saturable absorber (SA) in the far-field plane so as to non-linearly couple them. (b) Time evolution of the laser array intensity without the SA. (c) Time evolution with the SA indicating temporal Q switching.

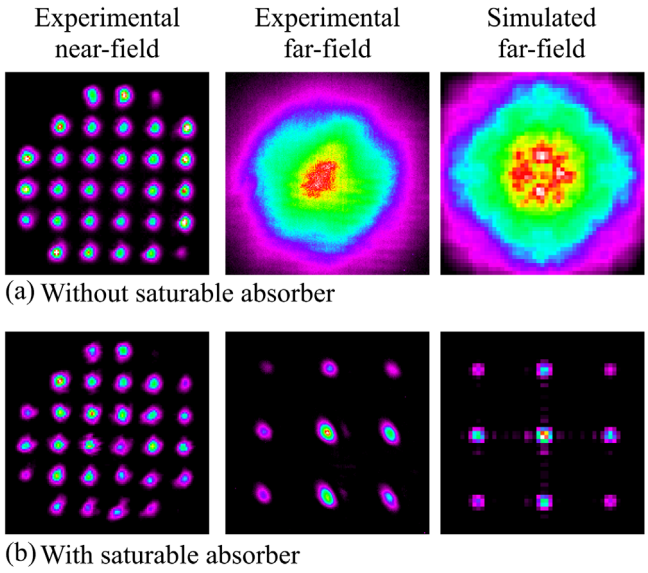

FIG. 2. Experimental and simulated near-field and far-field intensity distributions of the DCL arrangement. (a) Without and (b) with a SA in the far-field plane. The broad Gaussian far-field intensity distribution without the SA indicates that there is no phase relation between the lasers whereas the sharp peaks with the SA indicate near-perfect phase locking of the entire array. As evident, there is good agreement between the experimental results and the numerical simulations.

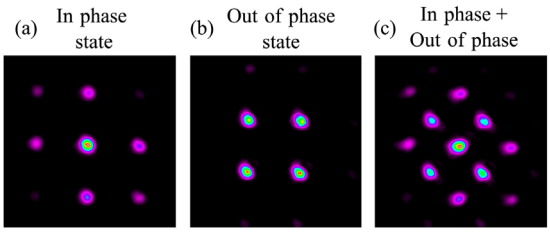

(d) Distribution of states for 50 pump pulse realizations.

Near lasing threshold	In phase state	Out of phase state	Coexistence states
Linear coupling	0	0	50
Nonlinear coupling	41	9	0

FIG. 3. Typical experimental far-field intensity distributions for different pump pulse realizations. (a) In phase state with SA, (b) out of phase state with SA and (c) coexistence state of in phase and out of phase states with SA. (d) Distribution of the number of states for 50 different pump pulse realizations, top row: linear coupling (Talbot diffraction), bottom row: nonlinear coupling (SA) near lasing threshold.

We determined the likelihood of the coexistence state when using either linear or nonlinear coupling. The results are presented in Fig. 3(d), for 50 different pump pulse realizations where all the near-field intensity distributions were the same. For the linear coupling (by Talbot diffraction with Talbot distance Z_T for which the two phase locked states are exactly degenerated), we always observed coexistence states only (top row). Such behavior can be easily understood: for linear coupling, the different longitudinal modes act as an ensemble of independent realizations, where each can have a different phase locked state. The probability that all of them have the same state is exponentially small. For linear coupling, the loss of the coexistence state is minimal, similar to that of in phase or out of phase state.

For nonlinear coupling (with SA), we found that the likelihood of the coexistence state is completely suppressed near the lasing threshold and all the longitudinal modes choose the same phase locked state (bottom row). Such suppression can be explained by noting that in the coexistence state, there are many far-field peaks whose intensity is relatively low and saturate less the SA, thereby increasing the loss. In addition, the nonlinear coupling between longitudinal modes provided by the SA forces the longitudinal modes to have the same phase locked state. As a result, near lasing threshold where mode competition is the strongest, a single phase locked state is enforced and the coexistence state is suppressed [32]. We also found that high above the lasing threshold, the likelihood of the coexistence state was not completely suppressed although it is lower with nonlinear coupling than with linear.

Next, we investigated whether adding nonlinear coupling to linearly coupled lasers can improve the convergence to the lowest loss phase locked state (e.g., out of phase state),

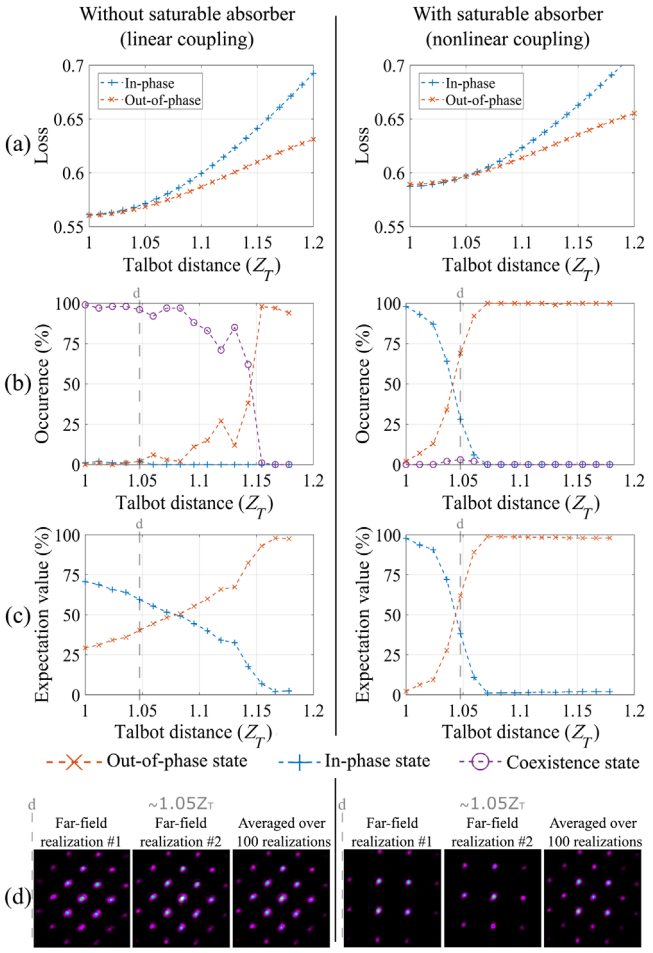

FIG. 4. The effect of the SA on the convergence to the lowest loss phase locked state. (a) Calculated losses of the in phase and out of phase states as a function of Talbot distance in the range $[1\text{to}1.2]Z_T$. The SA increases the loss of the out of phase state by $\sim 0.5\%$ as compared to the in phase state thereby shifting the degeneracy distance between them from $1Z_T$. to $1.05Z_T$. (b) Measured relative occurrence of the in phase, out of phase, and coexistence states as a function of Talbot distance. (c) Measured expectation value of the in phase and out of phase states as a function of Talbot distance. (d) Typical far-field intensity distribution for single realizations and averaged distribution over the 100 realizations at $1.05Z_T$.

when an additional state (e.g., in phase state) with nearly identical but slightly higher loss is present. The effects of the SA on the convergence to the lowest loss phase locked state are presented in Fig. 4. The linear losses of the in phase and out of phase states were controlled by varying the Talbot distance (round-trip distance between the near-field mask and the output coupler) [5].

Using an eigenvalues modal analysis [33], we calculated the losses, without and with a SA, of the in phase and out of phase states for different Talbot distances in the range $[1\text{to}1.2]Z_T$. The results are presented in Fig. 4(a). For linear coupling, there is a degeneracy between the two phase

locked states at $1Z_T$. The difference in loss between the two states increases as the Talbot distance increases, where the loss of the out of phase state becomes significantly lower [34]. When adding nonlinear coupling, the calculated losses of the in phase state are slightly reduced (by ~0.5%) compared with those of the out of phase state for all Talbot distances, shifting the degeneracy distance from $1Z_T$ to about $1.04Z_T$ [Fig. 4(a) right] [35].

We measured the relative occurrence of each phase locked state (in phase, out of phase, or coexistence state) as a function of the Talbot distance for 100 different pump pulse realizations [36]. The results are presented in Fig. 4(b). For linear coupling, the minimal loss phase locked state (i.e., out of phase state) with $\geq 90\%$ occurrence rate is achieved only at distances larger than $1.15Z_T$ where the loss difference between in phase and out of phase states is large [≃5% in Fig. 4(a) left]. For smaller loss difference, the coexistence state is dominant, indicating that some of the longitudinal modes select the wrong phase locked state.

For the nonlinear coupling, the occurrence of the coexistence state is negligible (occurs only around the degeneracy distance $1.04Z_T$ with a very small probability), confirming that with nonlinear coupling all longitudinal modes select the same phase locked state (as already noted in Fig. 3 without Talbot diffraction). As the Talbot distance is varied across the degeneracy distance $1.04Z_T$, a sharp transition occurs between the in phase and the out of phase states. The minimal loss state with $\geq 90\%$ occurrence rate is achieved at Talbot distances 1.03 and $1.06Z_T$ when the difference in loss is ≃0.2% (≃25 times smaller than for linear coupling). We also found that the results for the nonlinear coupling are more robust and repeatable [27].

The method used to obtain the results in Fig. 4(b) only provides the relative occurrence of each phase locked state and does not provide the ratio of intensities between the in phase and out of phase states. Figure 4(c) shows the expectation value of the in phase and out of phase states as a function of the Talbot distance (obtained by summing the far-field intensity distributions of all 100 realizations and calculating the expectation intensity value of each phase locked state).

For nonlinear coupling, the results in Figs. 4(b) and 4(c) have the same behavior (simply because there are only in phase or out of phase states with no coexistence state). For linear coupling, the minimal loss state with $\geq 90\%$ expectation value is achieved again only for Talbot distances larger than $1.15Z_T$, where the difference in loss is large (~5%). Even "majority selection" of the longitudinal modes (expectation value above 50%) fails for Talbot distances smaller than $1.08Z_T$, where the difference in loss is ≃1.3%. The improvement of nonlinear coupling over linear coupling for finding the lowest loss state can also be quantified by using the slope of the transition from the out of phase to in phase state, which is ≃5 times sharper with nonlinear coupling.

Finally, Fig. 4(d) shows experimental far-field intensity distributions at $1.05Z_T$ for two typical realizations and the averaged distribution over the 100 realizations, for both linear and nonlinear coupling. For linear coupling, the distributions for all the different single realizations are identical (and hence also is the averaged distribution) and correspond to the coexistence state, indicating that the longitudinal modes are uncoupled. For nonlinear coupling, the distribution for the single realizations correspond either to the in phase or out of phase state (no coexistence state), indicating that the longitudinal modes are coupled and the averaged distribution reveals both states. We also repeated the experiments for a larger range of Talbot distances and numerically simulated the far-field intensity distributions [27].

We calculated the loss functional that is minimized by the lasers at the vicinity of its global minimum [27]. Loss functionals for nonlinear coupling were theoretically investigated also for optical parametric oscillators and nonequilibrium condensates (polariton arrays) [9,19]. In polariton arrays, the nonlinear coupling introduced a phase lag in the system that shifted or destabilized the stationary point, with improved convergence to the ground-state solution [19].

We also showed analogy with strongly coupled Ising spins that produce significant magnetization even for magnetic energy smaller than their thermal energy [27].

To conclude, we showed that an array of 30 lasers can be phase locked efficiently and robustly, by resorting to nonlinear coupling with a saturable absorber in the far-field. The nonlinear coupling was found to significantly improve the ability of the lasers to converge to the correct minimal loss phase locked state, that is mapped to the ground state of the classical XY spin Hamiltonian [6]. It is 25 times more sensitive to differences in loss with five times faster convergence to the lowest loss state than with linear coupling. The nonlinear coupling forces all longitudinal modes of the lasers to have the same phase locked state.

We also showed that nonlinear coupling inherently improves the phase locking of many lasers. Specifically, reducing the sensitivity to misalignment errors, mechanical vibrations, thermal effects, and various aberrations. Moreover, nonlinear coupling also improves the phase locking by converging to a single (minimal loss) phase locking state. We plan to study the effect of nonlinear coupling on the time dynamics of the degenerate cavity laser after replacing the flash lamps pumping by diode pumping.

The authors wish to acknowledge the Israel Science Foundation and the Israeli Planning and Budgeting Committee Fellowship Program for their support.

*sim.mahler@gmail.com

[1] A. E. Siegman, *Lasers* (University Science Books, Mill Valey, California, 1986), 1st ed., Vol. 1, p. 1.
[2] A. F. Glova, Quantum Electron. **33**, 283 (2003).
[3] F. Kong, L. Liu, C. Sanders, Y. C. Chen, and K. K. Lee, Appl. Phys. Lett. **90**, 151110 (2007).
[4] S. Mahler, C. Tradonsky, R. Chriki, A. A. Friesem, and N. Davidson, OSA Continuum **2**, 2077 (2019).
[5] C. Tradonsky, V. Pal, R. Chriki, N. Davidson, and A. A. Friesem, Appl. Opt. **56**, A126 (2017).
[6] M. Nixon, E. Ronen, A. A. Friesem, and N. Davidson, Phys. Rev. Lett. **110**, 184102 (2013).
[7] S. Tamate, Y. Yamamoto, A. Marandi, P. McMahon, and S. Utsunomiya, arXiv:1608.00358.
[8] N. G. Berloff, M. Silva, K. Kalinin, A. Askitopoulos, J. D. Töpfer, P. Cilibrizzi, W. Langbein, and P. G. Lagoudakis, Nat. Mater. **16**, 1120 (2017).
[9] Y. Yamamoto, K. Aihara, T. Leleu, K. Kawarabayashi, S. Kako, M. Fejer, K. Inoue, and H. Takesue, npj Quantum Inf. **3**, 49 (2017).
[10] A. Marandi, Z. Wang, K. Takata, R. L. Byer, and Y. Yamamoto, Nat. Photonics **8**, 937 (2014).
[11] V. Pal, C. Tradonsky, R. Chriki, A. A. Friesem, and N. Davidson, Phys. Rev. Lett. **119**, 013902 (2017).
[12] S. Mahler, V. Pal, C. Tradonsky, R. Chriki, A. A. Friesem, and N. Davidson, J. Phys. B **52**, 205401 (2019).
[13] C. Tradonsky, I. Gershenzon, V. Pal, R. Chriki, A. A. Friesem, O. Raz, and N. Davidson, Sci. Adv. **5**, eaax4530 (2019).
[14] V. Eckhouse, M. Fridman, N. Davidson, and A. A. Friesem, Phys. Rev. Lett. **100**, 024102 (2008).
[15] Y. Zhou, L. Liu, C. Etson, Y. Abranyos, A. Padilla, and Y. C. Chen, Appl. Phys. Lett. **84**, 3025 (2004).
[16] J. Guillot, A. Desfarges-Berthelemot, V. Kermène, and A. Barthélémy, Opt. Lett. **36**, 2907 (2011).
[17] S. Sivaramakrishnan, W. Z. Chang, A. Galvanauskas, and H. G. Winful, IEEE J. Quantum Electron. **51**, 1 (2015).
[18] M. Nixon, O. Katz, E. Small, Y. Bromberg, A. A. Friesem, Y. Silberberg, and N. Davidson, Nat. Photonics **7**, 919 (2013).
[19] N. Stroev and N. G. Berloff, arXiv:1910.00842.
[20] M. Hercher, Appl. Opt. **6**, 947 (1967).
[21] A. K. Wojcik, N. Yu, L. Diehl, F. Capasso, and A. A. Belyanin, Opt. Eng. **49**, 1 (2010).
[22] H. G. Winful and D. T. Walton, Opt. Lett. **17**, 1688 (1992).
[23] E. Lacot and F. Stoeckel, J. Opt. Soc. Am. B **13**, 2034 (1996).
[24] X. Chen, Y. Bai, M. Jiang, L. Li, Y. Zhou, H. Wang, Z. Ren, and J. Bai, Appl. Phys. Express **5**, 122701 (2012).
[25] A. A. Ishaaya, N. Davidson, and A. A. Friesem, Opt. Express **13**, 4952 (2005).
[26] J. A. Arnaud, Appl. Opt. **8**, 189 (1969).
[27] See the Supplemental Material at http://link.aps.org/supplemental/10.1103/PhysRevLett.124.133901 for further calculated and experimental results, and technical details, which includes Refs. [1,5,6,28,29].
[28] H. E. Stanley, *Introduction to Phase Transitions and Critical Phenomena* (Oxford University Press, New York, 1971).
[29] J. Strecka and M. Jascur, Acta Phys. Slovaca **65**, 235 (2015).
[30] A. G. Fox and T. Li, Bell Syst. Tech. J. **40**, 453 (1961).
[31] R. W. Gerchberg and W. O. Saxton, Optik (Stuttgart) **35**, 237 (1972).
[32] The in phase state is the more dominant because it loss is slightly smaller than the out of phase state [as in Fig. 4(a)].
[33] D. Mehuys, W. Streifer, R. G. Waarts, and D. F. Welch, Opt. Lett. **16**, 823 (1991).
[34] To keep our system simple with only two low loss phase locked states, we suppressed two additional low loss phase locked states, see the Supplemental Material [27].
[35] The eigenvalues calculation uses saturation function for the SA that contains four parameters (SA's intensities and transmissions thresholds) that are adjusted to set the degeneracy distance to agree with the Talbot distance where the out of phase state intersects the in phase state in Figs. 4(b) and 4(c) that is about $1.04Z_T$.
[36] We analyzed the far-field intensity distribution of each realization and set an intensity threshold value (≈15% of the maximal intensity) for determining whether the in phase or out of phase or coexistence state is present.